NONCOHERENT EQUALIZATION ALGORITHMS BASED ON SEQUENCE ESTIMATION

Wolfgang H. Gerstacker, Robert Schober, and Johannes B. Huber

Lehrstuhl für Nachrichtentechnik II
Universität Erlangen-Nürnberg
Cauerstraße 7/NT, D-91058 Erlangen, Germany
e-mail: gersta@nt.e-technik.uni-erlangen.de

***Abstract* – Two noncoherent equalization algorithms are derived, which are based on sequence estimation. Better performance can be obtained than for noncoherent symbol–by–symbol equalizers known in literature. In the first scheme, the current received signal sample is multiplied by the previous complex–conjugated one like in a conventional differential detector prior to sequence estimation. Although this results in nonlinear intersymbol interference, the Viterbi algorithm (VA) can be employed for reconstruction of the data. The second algorithm is derived by modifying the optimum noncoherent sequence estimator, which is too complex for an implementation. The resulting scheme, which again applies the VA, can be interpreted as a generalization of multiple–symbol differential detection for the AWGN channel.**

1. INTRODUCTION

For transmission over additive white Gaussian noise (AWGN) or flat fading channels, differential detection (DD) of the received signal is often applied instead of coherent detection (CD). The major advantage of DD compared to CD is a reduced implementation complexity of the receiver because no synchronization of the carrier phase is required and also a certain offset in carrier frequency can be tolerated. In addition to that, DD has an improved resistance to fading. However, a loss in power efficiency results. E.g., DD of differentially encoded quaternary phase–shift keying (QDPSK) performs about 2 dB worse than CD at bit error rates (BERs) of practical interest. Several concepts have been proposed in literature in order to improve performance of DD, retaining its advantages. Perhaps the most important one is multiple–symbol (MS) DD, proposed by Divsalar and Simon [1]. In MSDD, maximum–likelihood sequence estimation (MLSE) of the transmitted phases is performed in multiple–symbol observation intervals. Varying the number of observations K, the gap between conventional DD, which can be seen as a special case of MSDD with $K = 2$, and CD can be filled. A substantial gain is possible, using only a few additional observations. E.g., power efficiency is improved by about 1.3 dB at BER $= 10^{-4}$ for $K = 5$. In the limit $K \to \infty$, the performance of CD is attained. Because the complexity of MSDD is considerably higher than that of DD, simplified approximate realizations are of interest. Several schemes have been proposed which reduce complexity by decision feedback, e.g. [2, 3, 4].

In contrast to AWGN and flat fading channels, only a few noncoherent receiver concepts are known for frequency–selective channels, producing intersymbol interference (ISI). In [5], adaptive linear equalization and differentially coherent reception are combined. However, high performance can only be obtained for channels, whose zeros are located not too close to the unit circle, which is often not the case in mobile communications. Especially for such channels, a scheme was proposed by Masoomzadeh-Fard and Pasupathy [6]. In [6], the current received signal sample is multiplied by the previous complex–conjugated one like in a differential detector after conversion to baseband. The resulting nonlinear ISI is equalized by a nonlinear equalizer using past decisions, which is designed by a Volterra series technique. Although the scheme performs significantly better than that of [5] for channels with severe amplitude distortions, the loss to coherent reception may be relatively large. Thus, there is room for further improvement.

In this paper, two novel noncoherent equalization algorithms based on sequence estimation are presented for M–ary DPSK. The organization of the paper is as follows. After a description of the system model in Section 2, the first algorithm is presented in Section 3, which applies sequence estimation to the output signal of a differential detector. Section 4 provides a derivation of the theoretically optimum noncoherent receiver, which, however, is not suited for an implementation. A second practical algorithm, using multiple–symbol observations for estimation of the transmitted sequence, is constructed in Section 5 by modifying the optimum receiver. Simulation examples given in Section 6 demonstrate the high performance of both algorithms.

2. TRANSMISSION MODEL

Fig. 1 shows a block diagram of the complex baseband system model under consideration. M–ary PSK symbols $b_k \in \mathcal{A} \triangleq \left\{ e^{j\frac{2\pi}{M}\mu} \mid \mu \in \{0, 1, \ldots, (M-1)\} \right\}$ are generated at the transmitter by differential encoding of M–ary DPSK symbols $a_k \in \mathcal{A}$: $b_k = a_k\, b_{k-1}$. The discrete–time received signal, sampled at times kT at the output of the receiver input filter, can be written

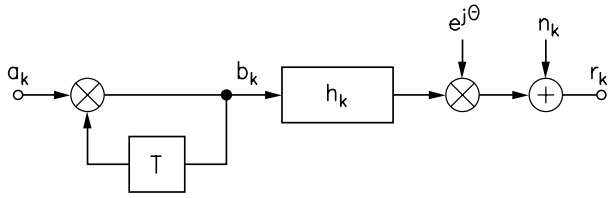

Figure 1: Block diagram of discrete–time transmission model.

as

$$r_k = \mathrm{e}^{j\Theta} \sum_{\kappa=0}^{L-1} h_\kappa \, b_{k-\kappa} + n_k. \tag{1}$$

Here, Θ denotes an unknown carrier phase, which is modelled as an uniformly distributed random variable in the interval $(-\pi, \pi]$. $\{h_k\}$ is the combined discrete–time impulse response of transmitter filter, channel, and receiver input filter; its length is denoted by L. We assume a square–root Nyquist frequency response for the receiver input filter (this includes a whitened matched filter [7] fitted to continuous–time transmit pulse and channel impulse response as a special case). Therefore, the complex Gaussian noise n_k with variance σ_n^2 is white.

In the receiver, the data sequence $\{a_k\}$ has to be recovered from the received sequence $\{r_k\}$.

3. EQUALIZATION BY SEQUENCE ESTIMATION AFTER DIFFERENTIAL DEMODULATION

In our first algorithm for noncoherent equalization, the nonlinear decision–feedback equalizer of [6] is replaced by a sequence estimator, which improves performance. A block diagram of the receiver is shown in Fig. 2. First, a signal

$$u_k = r_k \, r_{k-1}^* = y_k + z_k \tag{2}$$

is generated, where y_k denotes the useful component for sequence estimation, in which the unknown phase Θ is eliminated,

$$y_k = \sum_{\kappa=0}^{L-1} \sum_{\nu=0}^{L-1} h_\kappa \, h_\nu^* \, b_{k-\kappa} \, b_{k-1-\nu}^*, \tag{3}$$

and z_k an equivalent noise,

$$z_k = \mathrm{e}^{-j\Theta} \, n_k \sum_{\nu=0}^{L-1} h_\nu^* \, b_{k-1-\nu}^* + \mathrm{e}^{j\Theta} \, n_{k-1}^* \sum_{\kappa=0}^{L-1} h_\kappa \, b_{k-\kappa} + n_k \, n_{k-1}^*. \tag{4}$$

It can be shown by straightforward calculations, that z_k has zero mean and a covariance sequence $E\{z_{k+\lambda} \, z_k^*\} = \sigma_z^2 \, \delta_\lambda$, where δ_λ is the unit pulse sequence, i.e., $\delta_0 = 1$, $\delta_\lambda = 0$, $\lambda \neq 0$, and σ_z^2 denotes the variance of z_k, which is given by $\sigma_z^2 = 2 \, \sigma_n^2 \sum_{\kappa=0}^{L-1} |h_\kappa|^2 + \sigma_n^4$. However, $\{z_k\}$ is not a WGN sequence, because in general, the probability density function (pdf) of z_k is different from a Gaussian pdf. Theoretical considerations and simulations show, that the pdf strongly depends on the channel and σ_n^2. Also, in general, z_k and z_i, $k \neq i$, are only uncorrelated but not statistically independent. Nevertheless, for the following derivations $\{z_k\}$ is modelled as an i.i.d. Gaussian random sequence in order to obtain an algorithm suited for implementation. Although sequence estimation then is suboptimum and does not recover the maximum–likelihood sequence, an efficient algorithm results, as simulations will show later.

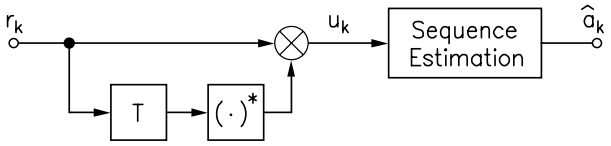

Figure 2: Receiver structure with differential demodulation and sequence estimation.

With the identity $b_\lambda \, b_\mu^* = \prod_{i=\mu+1}^{\lambda} a_i$, $\lambda, \mu \in \mathbb{Z}$, $\lambda > \mu$, and $|b_\lambda|^2 = 1$, the useful component can be decomposed into

$$y_k = \sum_{\kappa=0}^{L-1} |h_\kappa|^2 \, a_{k-\kappa} + \sum_{\nu=0}^{L-1} \sum_{\kappa=0}^{\nu-1} h_\kappa \, h_\nu^* \prod_{i=\kappa}^{\nu} a_{k-i} + \sum_{\kappa=0}^{L-1} \sum_{\nu=0}^{\kappa-2} h_\kappa \, h_\nu^* \prod_{i=\nu+1}^{\kappa-1} a_{k-i}^* + \sum_{\kappa=1}^{L-1} h_\kappa \, h_{\kappa-1}^*. \tag{5}$$

Obviously, y_k depends on L consecutive symbols a_k, $a_{k-1}, \ldots, a_{k-(L-1)}$. Defining a state vector $S_k \triangleq \left[a_{k-1} \; a_{k-2} \; \ldots \; a_{k-(L-1)}\right]$, and a transition vector between two states S_k and S_{k+1}, $\xi_k \triangleq \left[a_k \; a_{k-1} \; a_{k-2} \; \ldots \; a_{k-(L-1)}\right]$, the useful component can be modelled as output sequence of a finite state machine with input sequence $\{a_k\}$ and state vector sequence $\{S_k\}$. The current output $y_k = f(\xi_k)$ is uniquely determined by a_k and S_k, i.e., the state transition, with a function $f(\cdot)$ according to Eq. (5), and the new state S_{k+1} also results from a_k and S_k. If the output sequence was impaired by an AWGN sequence $\{z_k\}$, a maximum–likelihood estimate for the input sequence could be determined similar to the coherent case, for which the solution was given by Forney in [7]. This means, the Viterbi algorithm (VA) can be applied to a trellis diagram with M^{L-1} states and M transitions emerging from each state for minimization of the metric , $_1 \triangleq \sum_k \left| u_k - f(\tilde{\xi}_k) \right|^2$, with $\tilde{\xi}_k \triangleq \left[\tilde{a}_k \; \tilde{a}_{k-1} \; \tilde{a}_{k-2} \; \ldots \; \tilde{a}_{k-(L-1)}\right]$, where $\tilde{a}_{k-\mu}$ denote the trial symbols of the equalizer. The only difference to the coherent case is a modified function $f(\cdot)$, which describes nonlinear ISI due to differential demodulation instead of linear one, resulting in different branch metrics for the VA.

In our case the noise is neither Gaussian nor i.i.d. and also depends on the data sequence. Therefore the

described algorithm in general does not deliver the maximum–likelihood sequence, but promises significant improvement compared to symbol–by–symbol detection. This is confirmed by the simulation results of Section 6.

For an AWGN channel, i.e., $L = 1$ and $h_0 = 1$, Eq. (5) yields $y_k = a_k$, which means, that a trellis with only one state results, i.e., symbol–by–symbol decisions are performed after DD. Thus, the differential detector for the AWGN channel results as a special case.

Finally, it should be noted, that a similar scheme was proposed in [8] by Safavi and Lopes for application in DECT, in which the length of the overall impulse response is limited to $L = 2$ and GMSK modulation is applied instead of DPSK.

4. OPTIMUM NONCOHERENT EQUALIZATION

In this section, we derive the optimum (maximum–likelihood) noncoherent equalization algorithm for a transmission of data blocks, during which channel impulse response and phase Θ are assumed to be constant. In contrast to the first algorithm, DD is avoided, because otherwise optimum sequence estimation is very complex, as has been shown in Section 3.

We consider a transmission of $(N+1)$ PSK symbols $b_0, b_1, \ldots, b_N$, with $b_k = b_0 \prod_{i=1}^{k} a_i$, $1 \le k \le N$. Here, b_0 represents the reference phase, which can be chosen arbitrary. In order to guarantee a known initial and final state of the channel, $L-1$ zero symbols are transmitted prior to and after the data block. For estimation of $\{a_k\}$, $1 \le k \le N$, $N+L$ received samples r_k, $0 \le k \le N+L-1$, given by Eq. (1) have to be processed, which are collected in a vector $\boldsymbol{r} \triangleq [r_0\ r_1\ \ldots\ r_{N+L-1}]$. For the following, the received signal is decomposed into $r_k = \mathrm{e}^{j\Theta}\, y_k + n_k$, where the useful sequence $\{y_k\}$ now is generated by differential encoding of the DPSK sequence $\{a_k\}$ and subsequent convolution with the channel impulse response, cf. Section 2. Also, an integer number $m \in \{0, 1, \ldots, M^N - 1\}$ is assigned to each of M^N possible DPSK sequences $\{a_k\}$. The useful sequence corresponding to the data sequence with number m is denoted by $\{y_{k,m}\}$.

Now, the task of an optimum equalizer is to select that one out of all trial sequences $\{\tilde{a}_k\}$, or equivalently that number m, which maximizes the conditional pdf $p(\boldsymbol{r}|m)$. This is a special case of the general problem of deriving an optimum demodulator for signals with random, uniformly distributed phase in additive white Gaussian noise, for which the solution has been given in [9], pp. 350-352. According to Eq. (4C.9) of [9], the conditional pdf can be calculated as

$$p(\boldsymbol{r}|m) \sim \exp\left(-\frac{1}{\sigma_n^2} \sum_{k=0}^{N+L-1} \left(|r_k|^2 + |y_{k,m}|^2\right)\right) \cdot \mathrm{I}_0\left(\frac{2}{\sigma_n^2}\left|\sum_{k=0}^{N+L-1} r_k\, y_{k,m}^*\right|\right), \quad (6)$$

where $I_0(\cdot)$ is the zeroth order modified Bessel function of the first kind. Instead of $p(\boldsymbol{r}|m)$, also $\log\left(p(\boldsymbol{r}|m)\right)$ can be considered for maximization. This leads to the decision rule

$$\hat{m} = \underset{m}{\operatorname{argmin}} \left\{ \frac{1}{\sigma_n^2} \sum_{k=0}^{N+L-1} |y_{k,m}|^2 - \log\left(\mathrm{I}_0\left(\frac{2}{\sigma_n^2}\left|\sum_{k=0}^{N+L-1} r_k\, y_{k,m}^*\right|\right)\right)\right\}. \quad (7)$$

For an AWGN channel $|y_{k,m}| = 1, \forall\, k,\ m$ is valid, if PSK symbols are transmitted. Then, all sequences $\{y_{k,m}\}$ have equal energy, and the first term in argmin$\{\cdot\}$ in Eq. (7) can be omitted. Since $\log(I_0(\cdot))$ is a monotonically increasing function, Eq. (7) becomes equivalent to

$$\hat{m} = \underset{m}{\operatorname{argmax}} \left\{ \left|\sum_{k=0}^{N+L-1} r_k\, y_{k,m}^*\right| \right\}, \quad (8)$$

a result which has also been presented in [1, 10].

In the presence of ISI, different useful sequences in general also have different energy, and Eq. (8) cannot be used. However, a simplification of Eq. (7) is possible, applying the approximation $\log\left(\mathrm{I}_0(x)\right) \approx x - 2.4$, $x > 6$, which results in a decision rule independent of σ_n^2, being justified for moderate to high SNRs:

$$\hat{m} = \underset{m}{\operatorname{argmin}} \left\{ \sum_{k=0}^{N+L-1} |y_{k,m}|^2 - 2\left|\sum_{k=0}^{N+L-1} r_k\, y_{k,m}^*\right| \right\}. \quad (9)$$

Notice, that the reference phase b_0 has no influence on each of the presented rules Eq. (7), Eq. (8), and Eq. (9), as was to be expected for noncoherent equalization, and that recursive optimization is impossible for each of them. Thus, metrics have to be calculated for each possible DPSK sequence, resulting in a complexity growing exponentially with N. This excludes large blocks or continuous transmission. A further problem is, that only much smaller phase drifts can be tolerated than in the first algorithm, because a constant phase during the whole block has been assumed. In the first algorithm, the phase only has to be constant over two consecutive intervals. Both drawbacks can be circumvented by modifying the optimum algorithm, as will be shown in Section 5.

5. EQUALIZATION BY SEQUENCE ESTIMATION USING MULTIPLE–SYMBOL OBSERVATIONS

According to the previous section, optimum noncoherent sequence estimation is difficult to implement because its metric cannot be calculated recursively, which prohibits application of the VA. Therefore, instead of the metric of Eq. (9), the suboptimum version

$$,_2(m) \triangleq \sum_{\nu=0}^{N_s-1} \left(\sum_{k=\nu K}^{(\nu+1)K-1} |y_{k,m}|^2 - 2\left|\sum_{k=\nu K}^{(\nu+1)K-1} r_k\, y_{k,m}^*\right| \right) \quad (10)$$

is considered as a first approach. Obviously, the received signal is partitioned into N_s subblocks of length $K \geq 2$, with $N_s K = N + L$. To each of them, the optimum metric is applied, and finally the results are summed up. Notice, that the optimum metric in Eq. (9) and that of Eq. (10) deliver the same result for that number m corresponding to the data sequence actually transmitted, if noise is absent and Θ is constant for $0 \leq k \leq N + L - 1$. However, further modifications are necessary, as can be seen, if Eq. (10) is analyzed for an AWGN transmission. Here, decisions can be made separately for the different subblocks. It is straightforward to show, that the subblock metrics are independent of the assumed subblock reference phases $\tilde{b}_{\nu K}$, which means, that for any subblock ν and a given sequence $\{\tilde{b}_{\nu K}, \tilde{b}_{\nu K+1}, \ldots, \tilde{b}_{(\nu+1)K-1}\}$, at least $M-1$ different trial sequences exist exhibiting the same metric, which can be constructed by a rotation of the given sequence by a factor of $e^{j\frac{2\pi}{M}\mu}$, $\mu \in \{1, 2, \ldots, (M-1)\}$. Hence, in general, a wrong decision will be made upon the DPSK symbols $a_{\nu K}$ corresponding to the block limits. Therefore, an overlapping of consecutive subblocks by one symbol is introduced,

$$, \,'_2(m) \triangleq \sum_{\nu=0}^{N'_s-1} \left(\sum_{k=\nu(K-1)}^{(\nu+1)(K-1)} |y_{k,m}|^2 - 2 \left| \sum_{k=\nu(K-1)}^{(\nu+1)(K-1)} r_k \, y^*_{k,m} \right| \right), \tag{11}$$

resulting in N'_s subblocks, with $N'_s(K-1) = N+L-1$. (Notice, that this condition in general requires a slightly different block size than in the first approach.) Again, detection can be done on a subblock–by–subblock basis for the AWGN channel, in the course of which now the last phase estimate of the currently detected subblock $\hat{b}_{(\nu+1)(K-1)}$ serves as a reference phase for the next subblock $\nu+1$, resolving the ambiguity described above. A comparison with [1] shows immediately, that for the special case of an AWGN channel, the scheme is identical to MSDD and therefore can be interpreted as a generalization of the latter to ISI channels.

In the following, it is described how the metric $, \,'_2(m)$ can be minimized recursively by the VA. To each subblock, a state vector consisting of assumed symbols (equalizer trial symbols) is assigned, $\tilde{S}_\nu \triangleq [\tilde{a}_{\nu(K-1)} \; \tilde{a}_{\nu(K-1)-1} \; \ldots \; \tilde{a}_{\nu(K-1)-(L-2)}]$. Also, trial *hypersymbols* $\tilde{q}_\nu \triangleq [\tilde{a}_{(\nu+1)(K-1)} \; \tilde{a}_{(\nu+1)(K-1)-1} \; \ldots \; \tilde{a}_{\nu(K-1)+1}]$ are introduced. With these definitions, the metric increments (branch metrics) in Eq. (11) only depend on the assumed state and hypersymbol:

$$\begin{aligned}
&\lambda(\nu, \tilde{S}_\nu, \tilde{q}_\nu) \quad \triangleq \\
&\triangleq \sum_{k=\nu(K-1)}^{(\nu+1)(K-1)} |y_{k,m}|^2 - 2 \left| \sum_{k=\nu(K-1)}^{(\nu+1)(K-1)} r_k \, y^*_{k,m} \right| \\
&= \sum_{k=\nu(K-1)}^{(\nu+1)(K-1)} \left| \sum_{\kappa=0}^{L-1} \left(h_\kappa \, \tilde{b}_{\nu(K-1)-(L-1)} \prod_{i=\nu(K-1)-(L-2)}^{k-\kappa} \tilde{a}_i \right) \right|^2 \\
&\quad -2 \left| \sum_{k=\nu(K-1)}^{(\nu+1)(K-1)} r_k \sum_{\kappa=0}^{L-1} \left(h^*_\kappa \, \tilde{b}^*_{\nu(K-1)-(L-1)} \prod_{i=\nu(K-1)-(L-2)}^{k-\kappa} \tilde{a}^*_i \right) \right| \\
&= \sum_{k=\nu(K-1)}^{(\nu+1)(K-1)} \left| \sum_{\kappa=0}^{L-1} \left(h_\kappa \prod_{i=\nu(K-1)-(L-2)}^{k-\kappa} \tilde{a}_i \right) \right|^2 \\
&\quad -2 \left| \sum_{k=\nu(K-1)}^{(\nu+1)(K-1)} r_k \sum_{\kappa=0}^{L-1} \left(h^*_\kappa \prod_{i=\nu(K-1)-(L-2)}^{k-\kappa} \tilde{a}^*_i \right) \right|,
\end{aligned} \tag{12}$$

where $y_{k,m} = \sum_{\kappa=0}^{L-1} h_\kappa \, \tilde{b}_{k-\kappa}$ and the differential encoding rule have been used. The reference phase $\tilde{b}_{\nu(K-1)-(L-1)}$ could be eliminated in the final expression because of its independence of both summation variables k and κ. Hence, the total metric can be written as $, \,'_2(m) = \sum_{\nu=0}^{N'_s-1} \lambda(\nu, \tilde{S}_\nu, \tilde{q}_\nu)$, where trial hypersymbols corresponding to different subblocks can be chosen independently. Also, the new state $\tilde{S}_{\nu+1}$ is uniquely determined by $\tilde{S}_\nu$ and $\tilde{q}_\nu$. In summary, all conditions for an application of the VA [11] are satisfied. The corresponding trellis exhibits M^{L-1} different states $\tilde{S}_\nu$ for each ν, i.e., the same number as for MLSE in the coherent case [7]. (Termination effects in the neighbourhood of the block limits $k = 0$ and $k = N$ are neglected.) M^{K-1} branches run into each state, and also M^{K-1} branches emanate from each state. Thus, a total number of M^{L+K-2} branches have to be processed in each step of the VA, i.e., $M^{L+K-2}/(K-1)$ branches per decided symbol $\hat{a}_k$, and in general, a larger complexity results than for coherent MLSE, which requires processing of M^L branches per symbol [7].

For a further analysis of the trellis structure, two different cases have to be distinguished:

- $K > L$: For each of M^{2L-2} allowed state pairs $(\tilde{S}_\nu, \tilde{S}_{\nu+1})$, M^{K-L} different parallel transitions exist, because there are $K-L$ distinct trial symbols $\tilde{a}_{(\nu+1)(K-1)-(L-1)}, \tilde{a}_{(\nu+1)(K-1)-L}, \ldots, \tilde{a}_{\nu(K-1)+1}$ of the hypersymbol $\tilde{q}_\nu$ which do not appear in $\tilde{S}_{\nu+1}$. Out of each set of M^{K-L} parallel transitions, that one with minimum branch metric is selected and further considered in the VA, similar to decoding of trellis–coded modulation [12].

- $K \leq L$: Each trial symbol of the hypersymbol also appears in $\tilde{S}_{\nu+1}$, and only one transition per each of M^{L+K-2} allowed state pairs exist.

As a consequence of the applicability of the VA, also continuous transmission can now be admitted, if a decision delay ν_0 is introduced which has to be chosen large enough [11]. Then, a hard decided hypersymbol $\hat{q}_{\nu-\nu_0}$ is delivered by the VA at each step ν.

It should be mentioned, that for derivation of the above algorithm, it is sufficient that the phase Θ is constant in blocks only of length K. Therefore, it is expected, that much larger phase drifts can be tolerated in practice than for optimum noncoherent equalization

described in Section 4. Finally, we indicate, that the algorithm exhibits certain similarities to a decoding algorithm for noncoherent coded modulation for the AWGN channel, proposed by Raphaeli in [13]. Both algorithms perform sequence estimation using multiple–symbol observations. Their major differences consist in trellis and metric definition. Furthermore, in the approach in [13], in general, the observations overlap in more than one symbol. This could be also introduced here, improving performance, but further increasing complexity.

6. SIMULATION RESULTS

For performance assessment of our two algorithms, which in the following are denoted as DDSE (differential demodulation and sequence estimation) and MSSE (multiple–symbol sequence estimation), respectively, we first assume an $M = 4$–ary DPSK (QDPSK) transmission over a time–invariant channel with $L = 2$ proposed in [6], with $h_0 = h_2 = 0.304$, $h_1 = 0.903$. According to Fig. 7 of [6], for binary DPSK (BDPSK), equalization with nonlinear Volterra–based DFE requires an E_b/N_0 ratio (E_b denotes the (mean) received bit energy and N_0 the noise power spectral density) of $10\log_{10}(E_b/N_0) = 17$ dB for this channel, if a bit error rate of BER $= 10^{-4}$ is prescribed. Fig. 3 shows, that for this bit error rate, only 14.2, 13.7 and 12.5 dB are required for DDSE, MSSE ($K = 2$) and MSSE ($K = 3$), respectively. Taking into account that QDPSK in principle is less power efficient than BDPSK, a gain of at least 3 dB results in our scenario for all three algorithms, compared to that of [6]. Obviously, MSSE is better than DDSE irrespective of K, perhaps because the latter relies on less realistic approximations. Using MSSE, a gain of 1.2 dB can be obtained, increasing K from 2 to 3, which means, that the number of branch metric computations is doubled ($K = 2$ ($K = 3$): 64 (128) computations per QDPSK symbol). The complexity of MSSE ($K = 2$) in general is comparable to that of DDSE. For comparison, Fig. 3 also shows the performance of coherent MLSE [7] applied to differentially encoded QPSK transmitted via the given channel, which is about 3.1 dB better than MSSE ($K = 3$) at BER $= 10^{-4}$.

As a second example, we consider a $\pi/4$–shifted QDPSK transmission, which e.g. is applied in the IS-54 (IS-136) digital cellular standard, again over a time–invariant channel of [6] with $L = 2$, given by $h_0 = h_2 = 0.407$, $h_1 = 0.815$. Without loss of generality, the discrete–time received signal of a $\pi/4$–shifted QDPSK transmission over an ISI channel $\{h_k\}$ can first be multiplied by a factor $\mathrm{e}^{-jk\pi/4}$. Using straightforward manipulations, it then can be shown that the scheme can be modelled equivalently as a QDPSK transmission over a channel with impulse response $\{\mathrm{e}^{-jk\pi/4}h_k\}$. Hence, the derived equalization algorithms for DPSK can be directly used. Fig. 4 again shows, that MSSE is superior to DDSE. At BER $= 10^{-4}$, MSSE ($K = 3$) is 1.8 dB better than MSSE ($K = 2$) and 3.4 dB worse than coherent MLSE.

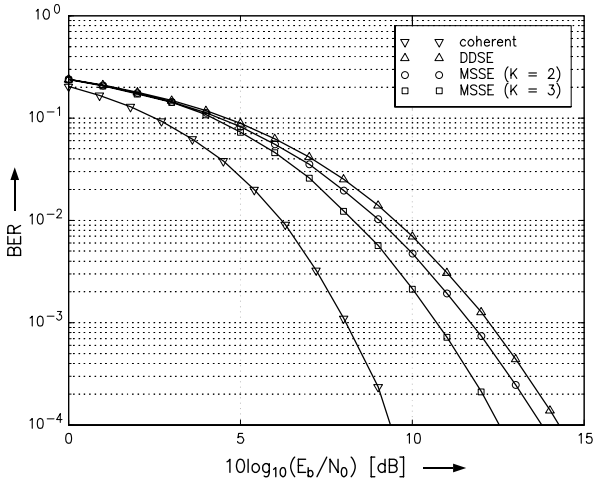

Figure 3: BER vs. E_b/N_0 for QDPSK modulation and $\{h_k\} = \{0.304, 0.903, 0.304\}$, using different equalization algorithms.

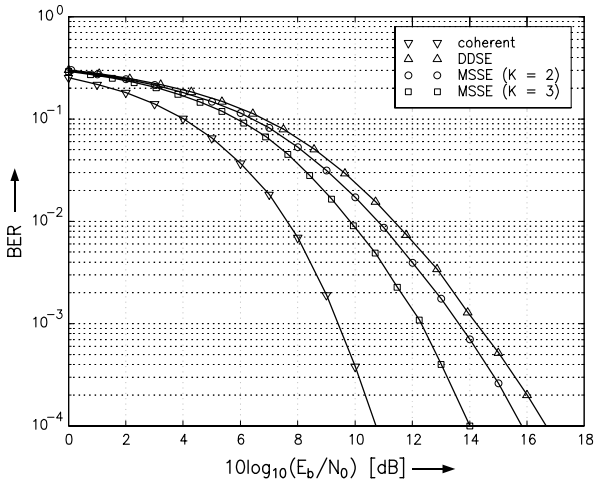

Figure 4: BER vs. E_b/N_0 for $\pi/4$–shifted QDPSK modulation and $\{h_k\} = \{0.407, 0.815, 0.407\}$, using different equalization algorithms .

Next, the effects of an uncompensated phase drift, caused by a demodulator frequency offset Δf which can be modelled by multiplication of r_k by $\mathrm{e}^{-j2\pi\Delta f\,k\,T}$, are examined for the same scenario. For the results of Fig. 5, which are valid for $10\log_{10}(E_b/N_0) = 10$ dB, the symbol interval of IS-54 ($T = 41.2\,\mu s$) has been assumed. The proposed algorithms degrade only slightly up to a frequency offset $\Delta f = 500$ Hz, which corresponds to a rotation by $7.4°$ per T. Additionally, the respective curves for an AWGN transmission have been included in Fig. 5. In contrast to these results, a coherent MLSE would degrade severely already for uncompensated offsets of a few Hz.

In a last example, the performance of the proposed algorithms is investigated for frequency–selective fading conditions. Again, an IS-54 transmission with $\pi/4$–shifted QDPSK and $T = 41.2\,\mu s$ is chosen. For derivation of the discrete–time channel model, transmitter

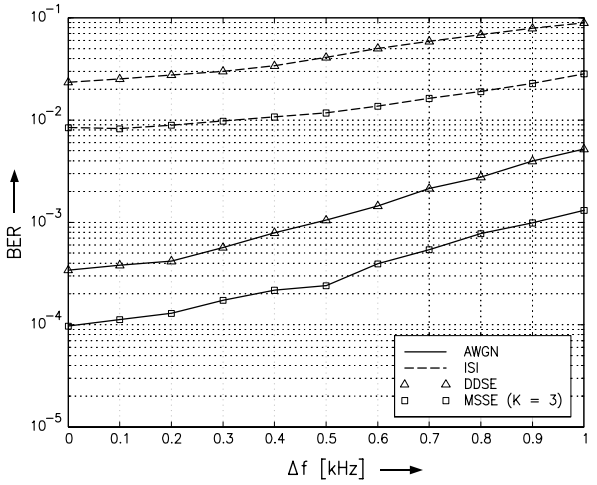

Figure 5: BER vs. Δf for $\pi/4$–shifted QDPSK transmission over a channel with $\{h_k\} = \{0.407, 0.815, 0.407\}$ and an AWGN channel, using different equalization algorithms ($10\log_{10}(E_b/N_0) = 10$ dB, $T = 41.2\,\mu s$).

and receiver input filters with square–root raised–cosine frequency response with roll–off factor 0.35 and a two–ray Rayleigh fading channel are assumed. The second ray of the channel is delayed by $T/4$ and attenuated by 3 dB with respect to the first ray, and the maximum Doppler frequency is 83.3 Hz. For simplicity, only the three main taps have been taken into account for simulations, i.e., $h_k = 0, k \notin \{0, 1, 2\}$. Also, availability of ideal channel state information in the receiver is assumed. Fig. 6 shows, that MSSE ($K = 3$) is 1.8 dB worse than coherent MLSE at BER $= 10^{-3}$, whereas DDSE is 3.6 dB worse.

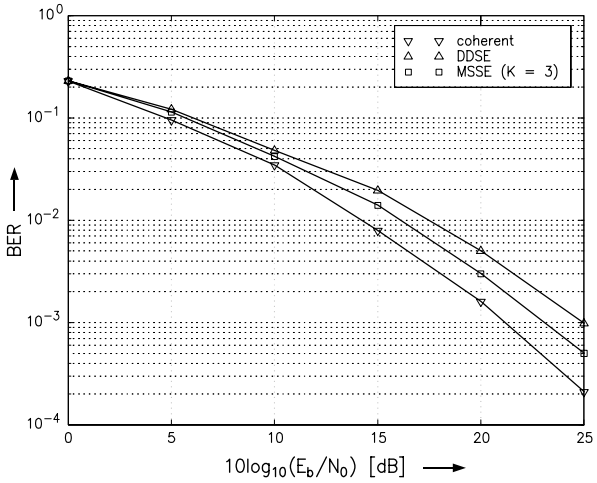

Figure 6: BER vs. E_b/N_0 for $\pi/4$–shifted QDPSK modulation and a two–ray Rayleigh fading channel, using different equalization algorithms.

7. CONCLUSIONS AND EXTENSIONS

In this paper, two noncoherent equalization algorithms based on sequence estimation have been introduced, which exhibit a higher performance than known techniques based on symbol–by–symbol decisions. The first algorithm can be interpreted as a generalization of common differential detection for the AWGN channel, while the second is equivalent to multiple–symbol differential detection, if ISI is absent. Performance results have been given for time–invariant and time–variant ISI channels, assuming knowledge of the channel impulse response at the receiver. The combination of the equalizers with suitable adaptation algorithms still has to be examined. Another topic for further research is complexity reduction, especially for the second algorithm. This might be accomplished by employing decision–feedback techniques proposed in [2, 3] in a per–survivor fashion [14].

REFERENCES

[1] D. Divsalar and M.K. Simon. Multiple–Symbol Differential Detection of MPSK. *IEEE Trans. on Commun.*, COM-38:300–308, March 1990.

[2] H. Leib and S. Pasupathy. The phase of a vector perturbed by Gaussian noise and differentially coherent receivers. *IEEE Transactions on Information Theory*, IT-34:1491–1501, November 1988.

[3] F. Edbauer. Bit Error Rate of Binary and Quaternary DPSK Signals with Multiple Differential Feedback Detection. *IEEE Trans. on Commun.*, COM-40:457–460, March 1992.

[4] N. Hamamoto. Differential Detection with IIR Filter for Improving DPSK Detection Performance. *IEEE Trans. on Commun.*, COM-44:959–966, August 1996.

[5] P. Sehier and G. Kawas Kaleh. Adaptive equaliser for differentially coherent receiver. *IEE Proceedings-I*, 137:9–12, February 1990.

[6] A. Masoomzadeh-Fard and S. Pasupathy. Nonlinear Equalization of Multipath Fading Channels with Noncoherent Demodulation. *IEEE Journal on Selected Areas in Communications*, SAC-14:512–520, April 1996.

[7] G.D. Forney, Jr. Maximum–Likelihood Sequence Estimation of Digital Sequences in the Presence of Intersymbol Interference. *IEEE Transactions on Information Theory*, IT-18:363–378, 1972.

[8] S. Safavi and L.B. Lopes. Simple non-coherent equalizer for the DECT system. *Electronics Letters*, 30(10):756–757, 1994.

[9] J.G. Proakis. *Digital Communications*. McGraw–Hill, New York, second edition, 1989.

[10] G. Colavolpe and R. Raheli. Non-Coherent Sequence Detection of M–ary PSK. In *Proceedings of the International Conference on Communications (ICC'97)*, pages 21–25, Montreal, June 1997.

[11] G.D. Forney, Jr. The Viterbi Algorithm. *IEEE Proceedings*, 61:268–278, 1973.

[12] G. Ungerböck. Trellis–Coded Modulation with Redundant Signal Sets, Part I. *IEEE Commun. Mag.*, 25:5–11, February 1987.

[13] D. Raphaeli. Noncoherent Coded Modulation. *IEEE Trans. on Commun.*, COM-44:172–183, February 1996.

[14] R. Raheli, A. Polydoros, and C.-K. Tzou. Per-Survivor Processing: A General Approach to MLSE in Uncertain Environments. *IEEE Trans. on Commun.*, COM-43:354–364, February/March/April 1995.